Interactions of the Acid and Base Catalysts on Staphylococcal Nuclease As Studied in a Double Mutant†

David J. Weber,‡ Alan K. Meeker, and Albert S. Mildvan*

Department of Biological Chemistry, The Johns Hopkins University School of Medicine, 725 North Wolfe Street, Baltimore, Maryland 21205

Received October 5, 1990; Revised Manuscript Received March 5, 1991

ABSTRACT: The mechanism of the phosphodiesterase reaction catalyzed by staphylococcal nuclease is believed to involve concerted general acid–base catalysis by Arg-87 and Glu-43. The mutual interactions of Arg-87 and Glu-43 were investigated by comparing kinetic and thermodynamic properties of the single mutant enzymes E43S (Glu-43 to Ser) and R87G (Arg-87 to Gly) with those of the double mutant, E43S + R87G, in which both the basic and acidic functions have been inactivated. Denaturation studies with guanidinium chloride, CD, and 600-MHz 1D and 2D proton NMR spectra, indicate all enzyme forms to be predominantly folded in absence of the denaturant and reveal small antagonistic effects of the E43S and R87G mutations on the stability and structure of the wild-type enzyme. The free energies of binding of the divalent cation activator Ca^{2+}, the inhibitor Mn^{2+}, and the substrate analogue 3′,5′-pdTp show simple additive effects of the two mutations in the double mutant, indicating that Arg-87 and Glu-43 act independently to facilitate the binding of divalent cations and of 3′,5′-pdTp by the wild-type enzyme. The free energies of binding of the substrate, 5′-pdTdA, both in binary E–S and in active ternary E–Ca^{2+}–S complexes, show synergistic effects of the two mutations, suggesting that Arg-87 and Glu-43 interact anticooperatively in binding the substrate, possibly straining the substrate by 1.6 kcal/mol in the wild-type enzyme. The large free energy barriers to V_{max} introduced by the R87G mutation ($\Delta G_1^* = 6.5$ kcal/mol) and by the E43S mutation ($\Delta G_2^* = 5.0$ kcal/mol) are partially additive in the double mutant ($\Delta G^*_{1+2} = 8.1$ kcal/mol). These partially additive effects on V_{max} are most simply explained by a cooperative component to transition state binding by Arg-87 and Glu-43 of −3.4 kcal/mol. The combination of anticooperative, cooperative, and noncooperative effects of Arg-87 and Glu-43 together lower the kinetic barrier to catalysis by 8.1 kcal/mol.

The enzyme staphylococcal nuclease is a Ca^{2+}-activated phosphodiesterase that catalyzes the hydrolysis of DNA and RNA to yield 3′-mononucleotides, accelerating the spontaneous rate of this reaction by a factor approaching 10^{16}-fold (Mildvan & Serpersu, 1989; Serpersu et al., 1987). Staphylococcal nuclease thus lowers the free energy of activation by 21.8 kcal/mol. The rate-limiting step in the enzyme-catalyzed reaction is probably the chemical step, a nucleophilic displacement at phosphorus of the leaving 5′-OH group of the polynucleotide by the entering hydroxyl group of water. The mechanism is likely to be associative and concerted, with a trigonal bipyramidal transition state (Figure 1), rather than an intermediate, based on our failure to detect such an intermediate by high-field ^{31}P NMR (<1% of the enzyme) (Weber et al., 1990a,b). From the effects of single mutations of active site residues on the kinetic, metal-binding, and substrate-binding properties of the enzyme, this one-step reaction is believed to involve concerted general acid–base catalysis by Arg-87 and Glu-43, respectively, with Arg-87 also contributing to transition-state stabilization. Acting together with enzyme-bound Ca^{2+}, these two residues contribute significantly to catalysis (Serpersu et al., 1987, 1989; Hibler et al., 1987).

In an attempt to dissect the quantitative factors responsible for the high catalytic power of staphylococcal nuclease, we have been studying the effects of double mutations of active site residues on the kinetic, metal-binding and substrate-binding properties of this enzyme (Weber et al., 1990b). In principle, the quantitative effect of a second mutation on a mutant enzyme may be antagonistic, absent, partially additive, additive, or synergistic with respect to the first mutation. We have recently found that a mutation of the general acid catalyst, R87G,[1] interacts differently with a mutation of a metal-liganding residue, D21E, in the R87G + D21E double mutant, depending on the kinetic or thermodynamic parameter measured. Thus, antagonistic effects of the two mutations on V_{max} were found and ascribed to antagonistic structural changes at the Ca^{2+}-binding site, since metal binding also showed antagonistic effects of the two mutations. In contrast, substrate binding showed simple additive weakening effects of the two mutations indicating the independent functioning of Arg-87 and Asp-21 in substrate binding, while binding of the substrate analogue 3′,5′-pdTp showed synergistic weakening effects of the two mutations in the double mutant, suggesting negative cooperativity or strain in the binding of the analogue by the wild-type enzyme (Weber et al., 1990b).

The present paper examines the interactions of the general acid catalyst Arg-87 with the general base catalyst Glu-43 by comparing the effects of the E43S and R87G single mutations with those of the E43S + R87G double mutant on V_{max}, on

† This work was supported in part by Grants DK28616 from the National Institutes of Health to Albert S. Mildvan and GM34171 to David Shortle.

* To whom correspondence should be addressed.

‡ National Institutes of Health postdoctoral fellowship (F32 GM13324).

[1] While the replacement of Arg-87 with Gly may be considered an extreme substitution, it should be noted that much more conservative substitutions for Arg-87, such as Lys or Cys, produce very similar kinetic effects as found with R87G and also weaken nucleotide binding as found with R87G. Thus the catalytic efficiency of R87K is 10^5-fold lower than that of the wild-type enzyme; substrate and pdTp binding are weaker (Pourmotabbed et al., 1990), and V_{max} of R87C is $>10^4$-fold lower than that of the wild-type enzyme, and pdTp binding is weaker (Mildvan & Serpersu, 1989). Hence it is unlikely that global structural changes are responsible for the observed effects of the R87G mutation.

0006-2960/91/0430-6103$02.50/0

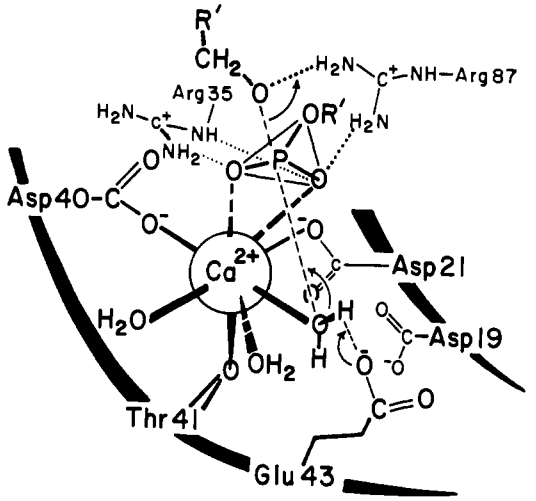

FIGURE 1: Transition state of the staphylococcal nuclease reaction based on the 1.5-Å X-ray structure (Cotton et al., 1979), kinetic studies (Anfinsen et al., 1971), and studies of active site mutants (Serpersu et al., 1987, 1988, 1989; Hibler et al., 1987; Weber et al., 1990b) showing an additional water ligand on Ca^{2+}, as found in the refined X-ray structure (Loll & Lattman, 1989). While an inner sphere water is depicted as attacking the phosphorus, a second sphere water molecule may be the substrate (Cotton et al., 1979).

enzyme stability, and on the binding of divalent cations, substrate, and the substrate analogue 3′,5′-pdTp. While the binding of divalent cations and of the substrate analogue 3′,5′-pdTp show simple additivity of the effects of these two mutations, synergistic effects on binding of the substrate 5′-pdTdA and partially additive effects on V_{max} are observed. These effects are most simply explained by assuming that Arg-87 and Glu-43 act independently to facilitate metal binding, interact anticooperatively to bind the substrate, and act cooperatively to bind the transition state.

Materials and Methods

Isolation of Enzymes. The preparation, isolation, and sequence analysis of all single mutations in the staphylococcal nuclease gene were carried out as previously reported (Shortle & Lin, 1985). All mutant proteins are designated by their amino acid changes relative to the wild-type enzyme, with the three symbol nomenclature in which the first letter designates the wild-type amino acid, the number designates the position of the amino acid, and the second letter designates the mutant amino acid substitution at that position. The double mutation was prepared by ligating *Ase*I restriction fragments from purified pFOG405 plasmids of the two single mutations E43S and R87G. The recombined DNA was identified by standard DNA sequencing methods (Shortle & Lin, 1985; Tabor & Richardson, 1987; Kunkel et al., 1987). Isolation of all mutant enzymes from an engineered strain of *Escherichia coli* that carries the lambda expression system were performed as described previously (Shortle & Meeker, 1989). All enzymes were purified to homogeneity as determined by SDS PAGE[2] (Laemmli, 1970) and by staining of the gels with Coomassie blue.

Quantitative Studies of Enzyme Stability. To quantitate the effects of mutations on the stability of staphylococcal nuclease, titrations with GnHCl were carried out, with monitoring of the decrease in fluorescence of the single Trp residue at position 140 as previously described (Shortle & Meeker, 1986). Linear plots of log K_{app}, the apparent equilibrium constant for protein denaturation, as a function of [GnHCl] were fit by least squares and extrapolated to zero denaturant concentration to yield limiting values of K_{app} and ΔG_F, the free energy of folding, in the absence of denaturant (Shortle et al., 1990).

Circular Dichroism Studies of Protein Structure. Circular dichroism spectra were recorded as previously described (Shortle & Meeker, 1989) at 20 °C in a nitrogen atmosphere on an AVIV 60DS spectropolarimeter using quartz cuvettes with a 0.1-mm path length. Samples contained 1.0 mg/mL wild-type or mutant enzyme, 1 mM sodium phosphate buffer, pH 7.0, and 100 mM NaCl. Spectra were the average of a series of five scans made at 1.0-nm intervals, with a 5-s integration time and 1.5-nm bandwidth and were corrected to an appropriate baseline scan obtained with buffer and salt alone. The secondary structures were estimated as previously described (Fry et al., 1988; Mullen et al., 1989) by comparing the experimental spectra with published CD basis sets (Chang et al., 1978; Compton & Johnson, 1986) using a multiple linear regression computer program. The best fits, judged by the difference between the calculated and experimental spectra, were obtained with the basis set of Chang et al. (1978). Extending this basis set from 190 to 185 nm, with the basis sets of Brahms & Brahms (1980), Stone et al. (1985), and Compton & Johnson (1986), did not significantly improve the fits but yielded better agreement of the secondary structure with that found in the X-ray structure of the wild-type enzyme.

Proton NMR Studies of Protein Structure. To determine if conformational differences exist between wild-type staphylococcal nuclease and the single and double mutants studied, E43S, R87G, and E43S + R87G, NMR spectra of each were obtained at 600 MHz in the absence and presence of 3′,5′-pdTp and Ca^{2+}. The samples were lyophilized twice from ^2H_2O. All samples containing enzyme alone (1.8 mM) also contained 30 mM NaCl, and 10 mM (d_{11}) Tris-DCl, pH* 7.0, in a total volume of 0.50 mL. Samples with Ca^{2+} and 3′,5′-pdTp contained 1.6 mM enzyme, 100 mM NaCl, 5.0 mM 3′,5′-pdTp, 31.0 mM $CaCl_2$, and 8.5 mM (d_{11}) Tris-DCl, pH* 7.0, in a total volume of 0.65 mL. Proton spectra at 600 MHz were obtained by collecting 32K data points over a spectral width of 10000 Hz with an acquisition time of 1.64 s. Saturation of the water or HDO resonance was performed in all cases by utilizing presaturation with low power (16 mW) from the decoupler. Two-dimensional NOE experiments (Jeener et al., 1979; Anil Kumar et al., 1980) were acquired in the phase-sensitive mode by using time-proportional phase incrementation (TPPI) (Marion & Wüthrich, 1983) with a 100-ms mixing time. Optimization of receiver phase was performed to remove baseline roll and to minimize baseline correction in F_2 (Marion & Bax, 1988). The parameters for acquisition of NOESY spectra included a 1.0-s relaxation delay, a 0.254-s acquisition time, an 8064-Hz sweep width, 4096 time domain data points in F_2, 1024 time domain data points in F_1, and a filter width of 30 KHz.

Both one-dimensional and two-dimensional data were processed on an Aspect 3000 computer using the standard Bruker software. For the two-dimensional spectra, the data were multiplied by a $\pi/6$ shifted squared sine bell prior to Fourier transformation in F_2. Linear baseline correction in F_2 was done on all slices, and the F_1 direction was Fourier transformed with zero filling to 2K data points. All chemical shifts are reported with respect to external DSS.

Enzyme Assays. For highly active enzymes (i.e., wild-type, E43S), the activity was measured by observing the absorbance

[2] Abbreviations: SDS, sodium dodecyl sulfate; PAGE, polyacrylamide gel electrophoresis; GnHCl, guanidinium chloride; CD, circular dichroism; pH*, pH measured in ^2H_2O; DSS, sodium 4,4-dimethyl-4-silapentanesulfonate.

increase at 260 nm as DNA is hydrolyzed (Cuatrecasas et al., 1967a,b). One unit of enzymatic activity is defined as the amount of enzyme causing a change of 1.0 absorbance unit per minute at 260 nm in a 1-cm cell. Protein concentrations for all enzymes were determined by the absorbance at 280 nm ($\epsilon^{0.1\%} = 0.93$) at neutral pH (Dunn et al., 1973). The assay mixture consisted of DNA (20–90 μg/mL), $CaCl_2$ (0.4–10.0 mM), and 40 mM Tris-HCl, pH 7.4, in a volume of 1.0 mL at 24 °C. To start the reaction, enzyme (0.045–0.054 μg of wild-type or 4.45 μg of E43S) was added. The velocity was determined from the linear portions of the recorder trace and expressed as the change in absorbancy per minute per microgram of protein. Enzymatic activities were linear with the amount of protein used in the assays. Analysis of the kinetic data for the wild-wild and E43S mutant enzymes was carried out as described previously (Serpersu et al., 1986, 1989).

For mutants such as R87G and the double mutant E43S + R87G with decreases in activity $\geq 10^4$ below that of the wild-type enzyme, two highly sensitive assays were used, as previously described (Weber et al., 1990b). In the first assay, which monitors the nicking of the supercoiled DNA, wild-type enzyme (0.80–131 pM) and mutants of staphylococcal nuclease diluted with 0.5 mg/mL BSA were incubated for 10 min in 20-μL solutions containing $CaCl_2$ (20.0 mM), negatively supercoiled plasmid DNA (1–282 μg/mL), and Tris-HCl (40 mM), pH 7.4, at 25 °C. The negatively supercoiled DNA (8.2 kb) consisted of pBR322 (3.7 kb), the immediate early simian cytomegalovirus, promoter (0.99 kb), and the 85% GC-rich Herpes simplex virus immediate early gene (3.5 kb), generously provided by M. Mullen and G. Hayward. The reaction was stopped by the addition of EDTA to give a final concentration of 45 mM, and the DNA was resolved by electrophoresis in agarose gel into two bands, the supercoiled DNA substrate and the nicked plus linearized product. The loss of the supercoiled substrate and the appearance of nicked and linearized products were quantitated by scanning a negative of the photographed gel with a scanning densitometer (Hoefer Scientific), analyzed as previously described (Weber et al., 1990b). The DNA concentrations in the incubation mixtures were varied over the range 1–287 μg/mL, and the data were plotted in double-reciprocal manner permitting extrapolation to obtain maximal velocities.

The second sensitive assay of staphylococcal nuclease, which gave nearly identical results, was based on the color change of a metachromatic dye from blue to pink upon the hydrolysis of DNA as the enzyme diffuses through a DNA-containing agar gel (Lachica et al., 1971; Shortle, 1983, 1986). This assay was also used to detect the low enzymatic activities of the R87G, E43S, and E43S + R87G mutants relative to the wild-type enzyme, as previously described (Serpersu et al., 1987, 1989; Weber et al., 1990b). A standard curve was generated by spotting the wild-type enzyme (0.1–20 ng) in 2-μL volumes onto a petri plate freshly prepared with 10 mL of agar gel containing 50 mM Tris-HCl, pH 7.4, 1% NaCl, 1% Difco agar, 300 μg/mL boiled salmon sperm DNA, 20 mM $CaCl_2$, and 0.2 mg/mL toluidine blue O. Plates were incubated for 3 h at 30 °C. Dilutions of mutant enzymes were adjusted to give halos equal in diameter to those produced by wild-type enzyme in order to compare relative activities.

Metal, Substrate, and Substrate Analogue Binding. The binding of Mn^{2+}, substrates, and substrate analogues to staphylococcal nuclease and its mutants was monitored by measuring the paramagnetic effects of Mn^{2+} on the longitudinal ($1/T_1$) relaxation rate of water protons, measured with a Seimco pulsed NMR spectrometer at 24.3 MHz with a 180°–τ–90° pulse sequence as previously described (Carr & Purcell, 1954; Mildvan & Engle, 1972). The observed enhancement of the relaxation rate is defined as $\epsilon^* = (1/T_{1P}^*)/(1/T_{1P})$ where $1/T_{1P}$ is the paramagnetic contribution to the relaxation rate in the presence (*) and absence of enzyme (Mildvan & Engle, 1972).

In independent Mn^{2+}-binding studies, the concentration of free Mn^{2+} in a mixture of free and bound Mn^{2+} was determined by electron paramagnetic resonance (Cohn & Townsend, 1954) with a Varian E-4 EPR spectrometer. The NMR and EPR data were analyzed as previously described (Mildvan & Cohn, 1963, 1966; Mildvan & Engle, 1972; Serpersu et al., 1986, 1987) to determine the stoichiometry (n) of Mn^{2+} bound to each enzyme, the dissociation constant (K_D), and the enhancement factor (ϵ_b) of the binary enzyme–Mn^{2+} complex. In addition, the binding of Mn^{2+} to enzyme–3′,5′-pdTp and enzyme–5′-pdTdA complexes was monitored by EPR and by changes in $1/T_{1P}^*$ of water protons, providing independent measurements of the dissociation constants (K_A') of Mn^{2+} from ternary complexes. Titrations of the binary enzyme–Mn^{2+} complexes with 3′,5′-pdTp and 5′-pdTdA monitoring changes in $1/T_{1P}$ of water protons were analyzed by computer as previously described (Reed et al., 1970; Mildvan & Engle, 1972; Serpersu et al., 1987) to give dissociation constants (K_3) and enhancement factors (ϵ_T) of ternary complexes. The dissociation constants for binary and ternary Ca^{2+} complexes were obtained by competition experiments in which the corresponding Mn^{2+} complex was titrated with Ca^{2+}, monitoring the displacement of Mn^{2+} by the decrease in the enhancement (ϵ^*) of $1/T_{1P}$ of water protons, and independently by the appearance of free Mn^{2+} in the EPR spectrum, as previously described (Serpersu et al., 1986, 1987).

Results

Kinetic Properties of the E43S + R87G Double Mutant Compared with the Individual Single Mutants of Staphylococcal Nuclease. We have previously pointed out that the quantitative effect of a second mutation on a kinetic or thermodynamic parameter of a mutant enzyme may be antagonistic, absent, partially additive, additive, or synergistic with respect to the effect of the first mutation (Weber et al., 1990b). The residual maximal activity of the E43S + R87G double mutant, relative to that of the wild-type enzyme, was determined by sensitive assays measuring both the extent of nicking of supercoiled DNA and the development of a halo due to DNA hydrolysis in an agar gel (Table I). While V_{max} of the R87G mutant is $10^{4.8\pm0.1}$-fold lower than that of the wild-type enzyme and E43S is $10^{3.7\pm0.3}$-fold lower, V_{max} of the E43S + R87G double mutant is only $10^{6.0\pm0.3}$-fold below that of the wild-type enzyme, and K_M is essentially unchanged. Thus, the loss in maximal activity in the double mutant, while greater than that with either single mutation alone, is not the product of each individual effect ($10^{8.5}$) but is $10^{2.5}$-fold smaller than this product.[3]

Expressed in terms of free energy (Table II), as is generally done (Carter et al., 1984; Knowles, 1987, Weber et al., 1990b), the more damaging single mutation R87G introduces a free energy barrier to V_{max} (ΔG^*_1) of 6.5 ± 0.1 kcal/mol, the E43S single mutation introduces a free energy barrier to V_{max} (ΔG^*_2) of 5.0 ± 0.4 kcal/mol, and together in the double mutant, they produce a free energy barrier to V_{max} (ΔG^*_{1+2}) of 8.1 ± 0.4 kcal/mol, which is 3.4 kcal/mol smaller than the sum of the

[3] This extra activity is unlikely to be due to genetic reversion to either of the single mutants since unreasonably high reversion rates of 0.5% (E43S) or 6.3% (R87G) would be required.

Table I: Factors of Decrease in V_{max} for Staphylococcal Nuclease Mutants Relative to the Wild-Type Enzyme[a]

mutant	assay: DNA hydrolysis[b]	assay: supercoil nicking[c]	assay: blue plate[d]	average
R87G		$10^{-4.7}$	$10^{-4.8}$	$10^{-4.8 \pm 0.1}$
E43S	$10^{-3.4}$		$10^{-4.0}$	$10^{-3.7 \pm 0.3}$
E43S + R87G		$10^{-6.3}$	$10^{-5.7}$	$10^{-6.0 \pm 0.3}$

[a] The wild-type enzyme utilized in each assay was also assayed by DNA hydrolysis to give 0.714 $\Delta A/(\mu g \cdot min)$ at pH 7.4 and 24 °C, which can be expressed as $k_{cat} = 95\ s^{-1}$ assuming the molecular weight of the substrate to be an average tetranucleotide (MW = 1400) and $\Delta A = 0.3$ for the complete hydrolysis of 50 μg/mL DNA (Cuatrecasas et al., 1967a,b; Serpersu et al., 1987). V_{max} for the wild-type enzyme was arbitrarily assigned the value 1 for comparison. [b] The data are from Serpersu et al., 1987. [c] The dilutions of the wild-type enzyme were adjusted to give bands of nicked DNA equal in amount to those produced by the mutant enzyme. K_M values of the supercoiled DNA were 354 ± 152 μg/mL with the wild-type enzyme and 503 ± 393 μg/mL with the E43S + R87G double mutant enzyme. [d] The dilutions of the wild-type enzyme were adjusted to give pink halos equal in diameter to those produced by the mutant enzyme.

individual effects. Therefore the effects on V_{max} of the R87G and E43S mutations are partially additive in the double mutant.

Table II records two important differences in free energy, $\Delta\Delta G^{\ddagger}_A$ and $\Delta\Delta G^{\ddagger}_B$, which are used for analyzing the effects of two mutations on the kinetic and thermodynamic parameters of enzymes (Weber et al., 1990b). The first difference $\Delta\Delta G^{\ddagger}_A = \Delta G^{\ddagger}_{1+2} - \Delta G^{\ddagger}_1$ measures the additional effect of the second mutation on the more damaging first mutation ($\Delta G^{\ddagger}_1$) in the double mutant ($\Delta G^{\ddagger}_{1+2}$). In the present case the $\Delta\Delta G^{\ddagger}_A$ value of 1.6 ± 0.4 kcal/mol is 3.4 kcal/mol lower than the effect of the second mutation alone ($\Delta G^{\ddagger}_2 = 5.0 \pm 0.4$ kcal/mol), emphasizing the partial additivity of the effects on V_{max}. The second difference $\Delta\Delta G^{\ddagger}_B = \Delta G^{\ddagger}_{1+2} - \Delta G^{\ddagger}_1 - \Delta G^{\ddagger}_2$ measures the departure from simple additivity of the effects of the two mutations on the wild-type enzyme. Since simple additivity results from independent effects of the two single mutations on the wild-type enzyme, $\Delta\Delta G^{\ddagger}_B$ is a measure of the interaction energy of the two residues in the wild-type enzyme (Weber et al., 1990b; Kuliopulos et al., 1990), which in the case of V_{max} is −3.4 ± 0.6 kcal/mol. This interaction may reflect cooperative stabilization of the transition state by Glu-43 and Arg-87.

Stability of Wild-Type and Mutants of Staphylococcal Nuclease. Titrations of the wild-type enzyme and the single and double mutant enzymes with GnHCl, in the absence of stabilizing divalent cations or substrate, revealed sigmoidal decreases in the fluorescence of Trp-140 in all cases. Half-maximal denaturation occurred at 0.44, 0.64, 0.80, and 0.95 M denaturant for the R87G mutant, the E43S + R87G double mutant, the wild-type enzyme, and the E43S single mutant, respectively, indicating protein stability to increase in this order (Figure 2A, Table III). Extrapolation of semilogarithmic plots of K_{app}, the apparent equilibrium constant for denaturation, to zero [GnHCl] as previously described (Figure 2B, Shortle & Meeker, 1986; Shortle et al., 1990) yielded limiting values of K_{app}, in the absence of GnHCl, which were used to calculate the free energies of folding ΔG_F in each case (Table III). Despite the differences in ΔG_F of the wild-type and mutant enzymes, it should be noted (Table III) that all enzyme forms are at least 99% folded in the absence of denaturant, i.e., under the conditions of the kinetic and ligand-binding studies.

As summarized in Table II, while the E43S mutation stabilizes the wild-type enzyme to GnHCl by −0.9 kcal/mol and the R87G mutation destabilizes the enzyme by 2.6 kcal/mol,

Table II: Changes in Free Energy of Activation and Binding (kcal/mol) by Staphylococcal Nuclease Resulting from the R87G, E43S, and E43S + R87G Mutations[a]

effect of mut 2 on mut 1	parameter[b]	ΔG_1	ΔG_2	ΔG_{1+2}	$\Delta\Delta G_A$ $(\Delta G_{1+2} - \Delta G_1)$	$\Delta\Delta G_B$ $(\Delta G_{1+2} - \Delta G_1 - \Delta G_2)$
antagonistic	K_{app}	2.7 ± 0.2	−0.9 ± 0.2	1.1 ± 0.2	−1.6 ± 0.3	−0.7 ± 0.3
none	K_3 (Mn, pdTdA)	2.7 ± 0.1	−0.7 ± 0.2	2.8 ± 0.2	0.1 ± 0.2	0.8 ± 0.3
	K_A' (Mn, pdTdA)	2.3 ± 0.2	0.7 ± 0.1	2.4 ± 0.2	0.1 ± 0.3	−0.6 ± 0.3
	K_3 (Ca, pdTp)	0.1 ± 0.5	−0.9 ± 0.4	0.2 ± 0.4	0.1 ± 0.6	1.0 ± 0.8
partially additive	V_{max}	6.5 ± 0.1	5.0 ± 0.4	8.1 ± 0.4	1.6 ± 0.4	−3.4 ± 0.6
additive	K_D (Ca)	1.3 ± 0.2	1.4 ± 0.2	2.3 ± 0.2	1.0 ± 0.3	−0.4 ± 0.4
	K_D (Mn)	0.4 ± 0.2	1.2 ± 0.1	1.6 ± 0.2	1.2 ● 0.3	0.0 ± 0.3
	K_A' (Ca, pdTp)	1.8 ± 0.2	0.7 ± 0.2	2.7 ± 0.2	0.9 ± 0.3	0.2 ± 0.4
	K_A' (Mn, pdTp)[c]	1.4 ± 0.2	−0.1 ± 0.3	1.2 ± 0.1	−0.2 ± 0.2	−0.1 ± 0.3
	K_A' (Ca, pdTdA)	2.0 ± 0.2	1.1 ± 0.2	3.0 ± 0.2	1.0 ± 0.2	−0.1 ± 0.3
	K_3 (Mn, pdTp)	0.6 ± 0.4	−1.4 ± 0.4	−0.5 ± 0.3	−1.1 ± 0.5	0.3 ± 0.6
	K_2 (Mn, pdTp)	1.0 ± 0.5	−0.2 ± 0.4	1.2 ± 0.5	0.2 ± 0.6	0.4 ± 0.8
	K_2 (Ca, pdTp)	1.4 ± 0.6	0.5 ± 0.6	2.5 ± 0.4	1.1 ± 0.7	0.6 ± 0.9
synergistic	K_S (pdTdA)	1.0 ± 0.2	−0.2 ± 0.2	2.2 ± 0.2	1.2 ± 0.3	1.4 ± 0.3
	K_3 (Ca, pdTdA)	1.7 ± 0.2	−0.4 ± 0.4	2.9 ± 0.3	1.2 ± 0.3	1.6 ± 0.5
	K_2 (Mn, pdTdA)	3.2 ± 0.2	0.5 ± 0.2	4.5 ± 0.1	1.3 ± 0.2	0.8 ± 0.3
	K_2 (Ca, pdTdA)	2.9 ± 0.2	1.0 ± 0.2	5.2 ± 0.2	2.3 ± 0.3	1.3 ± 0.4

[a] ΔG_1 and ΔG_2 are the effects of the R87G and E43S single mutants, respectively, and ΔG_{1+2} the effects of the E43S + R87G double mutation on the parameters of the wild-type enzyme. For V_{max}, free energies of activation ($\Delta G^{\ddagger}$) are meant. [b] Free energies of reciprocals of all equilibrium constants are shown for consistency so that positive values of ΔG for all parameters indicate damage to the enzyme. [c] K_A' (Mn, pdTp) could also be listed under "none" since $\Delta\Delta G_A \sim 0$. It is shown as additive for consistency with K_A' (Ca, pdTp).

Table III: Analysis of GnHCl Denaturation Studies of Wild-Type and Mutant Staphylococcal Nuclease

enzyme	$[GnHCl]_{1/2}$ (M)	relative slope	K_{app}[a]	% folded at [GnHCl] = 0	ΔG_F (kcal/mol)[a]
WT	0.80	1.00	$7.8 \pm 0.2 \times 10^{-5}$	99.99	−5.5 ± 0.1
E43S	0.95	0.97	$1.7 \pm 0.04 \times 10^{-5}$	99.998	−6.4 ± 0.1
R87G	0.44	0.91	$8.4 \pm 0.3 \times 10^{-3}$	99.17	−2.8 ± 0.1
E43S + R87G	0.64	1.00	$4.9 \pm 0.2 \times 10^{-4}$	99.95	−4.4 ± 0.1

[a] Errors in K_{app}, the equilibrium constant for denaturation at zero [GnHCl], and in ΔG_F, the free energy of folding, are ±2 SEM. T = 20 °C.

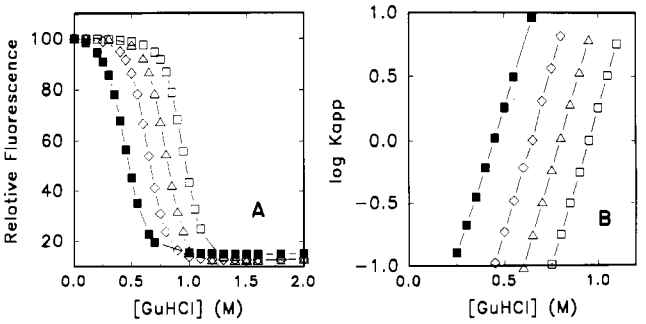

FIGURE 2: Denaturation of staphylococcal nuclease and its mutants by guanidinium chloride monitored by fluorescence of Trp-140. (A) Effect of GnHCl on the relative fluorescence of the wild-type enzyme (△), E43S (□), R87G (■), and the double mutant E43S + R87G (◇). Components present in a 2.0-mL volume were enzyme (40–50 γ/mL), sodium phosphate, pH 7.0 (25 mM), and NaCl (100 mM). A Spex Fluorolog II spectrophotofluorimeter was used with excitation at 295 nm and emission at 325 nm. T = 20 °C. (B) Linear plot of log K_{app}, the apparent equilibrium constant for denaturation, as a function of [GnHCl], used to determine the parameters in Table III. Conditions and symbols are as in panel A.

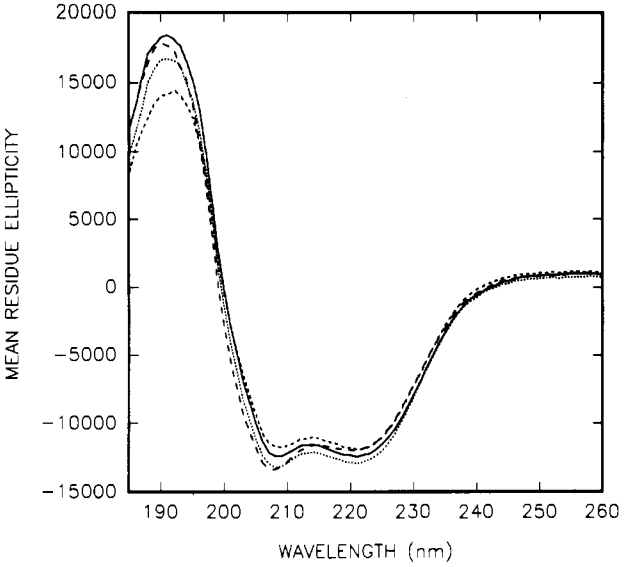

FIGURE 3: Circular dichroism spectra of wild-type and mutant forms of staphylococcal nuclease. Conditions are described under Materials and Methods. Wild type (—); E43S (– – –); R87G (- - -); E43S + R87G (···). The percent secondary structures, with standard deviations, estimated as described under Materials and Methods, were as follows: (Wild-type) α, 27 ± 2; β, 16 ± 1; turns, 16 ± 1; aperiodic, 41 ± 3. (R87G) α, 26 ± 3; β, 16 ± 2; turns, 14 ± 2; aperiodic, 44 ± 6. (E43S) α, 28 ± 3; β, 9 ± 1; turns, 23 ± 3; aperiodic, 40 ± 5. (Double mutant) α, 32 ± 5; β, 2 ± 1; turns 24 ± 4; aperiodic, 42 ± 7.

the double mutation destabilizes the enzyme by only 1.1 kcal/mol. This value is significantly lower than 1.8 kcal/mol, which would have been found if simple additivity of effects had occurred. This departure from additivity, or $\Delta\Delta G_B$ value of −0.7 kcal/mol, indicates that the E43S mutation antagonizes the destabilizing effect of the R87G mutation in the wild-type enzyme by 0.7 kcal/mol, presumably due to antagonistic structural effects on the enzyme. In accord with the present data, thermal denaturation studies of single mutants revealed stabilizing effects of the E43S mutation and destabilizing effects of the R87K mutation (Hibler et al., 1987; Pourmotabbed et al., 1990).

Structural Studies of Wild-Type and Mutants of Staphylococcal Nuclease by CD Spectroscopy. Consistent with the denaturation studies, CD spectra of the wild-type, R87G, E43S, and double mutant enzymes were very similar (Figure 3), revealing at most only slight changes in the overall secondary structures of the mutant enzymes from that of the wild-type. Thus, the helix contents of the R87G, E43S, and E43S + R87G double mutant were estimated to be 26 ± 3%, 28 ± 3%, and 32 ± 5%, respectively, indistinguishable from that of the wild-type enzyme, which was 27 ± 2%. Although agreement with the wild-type enzyme was also noted in the content of aperiodic structure, and in the sum of β-strands and turns (Figure 3), these elements of secondary structure are less reliably determined by CD spectroscopy.

Structural Studies of Wild-Type and Mutants of Staphylococcal Nuclease by ^1H NMR Spectroscopy. Most of the proton resonances in the NMR spectrum of wild-type staphylococcal nuclease complexed with Ca^{2+} and 3′,5′-pdTp have previously been assigned to specific residues (Torchia et al., 1989; Wang et al., 1990). Our NMR studies at 600 MHz both in the absence (Figure 4) and presence of Ca^{2+} and 3′,5′-pdTp (Figure 5) show all of the mutant enzymes to be highly structured, comparable to the wild-type enzyme. No significant conformation changes from the wild-type enzyme were detected in the E43S mutant and in the E43S + R87G double mutant, as reflected in negligible changes in chemical shifts for the upfield-shifted methyl resonances (≤0.02 ppm, Figures 4A and 5A) for the aromatic resonances (≤0.05 ppm, Figures 4B and 5B) and for side-chain and backbone resonances that are dipolar coupled to these signals (≤0.09 ppm) (not shown). No peaks disappeared and no new peaks appeared in these mutants. Such small variations in chemical shift are comparable to those seen among multiple preparations of the wild-type enzyme or of the same mutant (≤0.04 ppm).

Similarly, the R87G mutant, in the absence or presence of Ca^{2+} and 3′,5′-pdTp, showed minimal changes from the wild-type enzyme in the chemical shifts of the upfield methyl resonances (≤0.02 ppm, Figures 4A and 5A) and in their NOESY connectivities (not shown). However, in the NOESY spectrum of the R87G mutant alone, the aromatic resonances assigned in the wild-type enzyme by Torchia et al. (1989) to the δ and ε protons of Tyr-93 showed two resonances each, one pair at the same chemical shift as found with wild-type and the other pair shifted upfield by 0.22 and 0.14 ppm, respectively (Figure 4B), probably due to hindered ring flipping, since the backbone α and β proton resonances of Tyr-93 showed little or no change in chemical shift (≤0.02 ppm).

In the presence of Ca^{2+} and 3′,5′-pdTp, the aromatic proton resonances of R87G, assigned in the wild-type enzyme by Torchia et al. (1989) and Wang et al. (1990) to the δ and ε protons of Tyr-85 and Tyr-113 and to the δ protons of Tyr-115, also showed such additional resonances shifted by −0.16 to 0.08 ppm from those of the wild-type (Figure 5B). The backbone α and β proton resonances of these residues showed smaller or no changes in chemical shift (≤0.07 ppm) (not shown). Hence the aromatic region of the spectrum of the R87G mutant shows small conformational differences from the wild-type enzyme manifested by hindered flipping of one or three aromatic rings between two environments. These small conformational differences from the wild-type enzyme found in the R87G mutant were not detected in the E43S + R87G double mutant, qualitatively confirming the small antagonistic effects of the two mutations.

Binary Mn^{2+} and Ca^{2+} Complexes of the E43S + R87G Double Mutant. To further investigate the interactions of the two single mutations in the double mutant, metal- and substrate-binding studies were performed. The binary enzyme–Mn^{2+} complex of the double mutant E43S + R87G was examined by a direct titration of the enzyme with $MnCl_2$. At each point of the titration, the concentration of free Mn^{2+} was determined by EPR spectroscopy, and the enhancement (ε*)

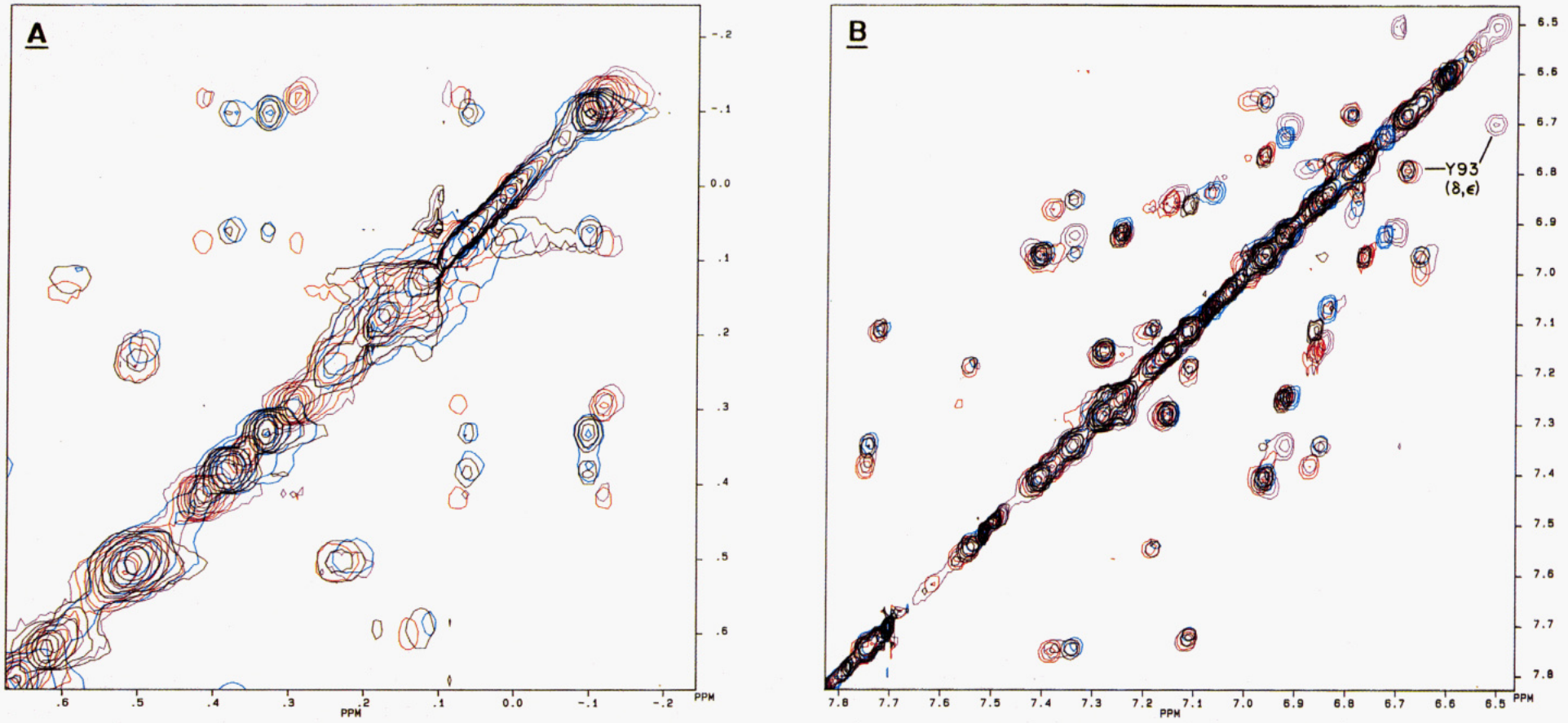

FIGURE 4: 2D ^1H NMR (phase-sensitive NOESY) spectra in ^2H_2O of wild-type staphylococcal nuclease (blue) and the following mutants: E43S (brown); R87G (purple); E43S + R87G (red). The upfield region (A) and the downfield aromatic region (B) are shown. In (B) the cross peak due to Tyr-93 was assigned on the basis of the sequential assignments in the ternary Ca^{2+}–3′,5′-pdTp complex of the wild-type enzyme (Torchia et al., 1989; Wang et al., 1990). In the absence and presence of Ca^{2+} and 3′,5′-pdTp, the chemical shifts of the α, β, β_2, δ, and ϵ protons of Tyr-93 remained unchanged (±0.01 ppm). An additional cross peak for Tyr-93 is noted with the R87G mutant (see Results). Concentrations and experimental conditions are given under Materials and Methods.

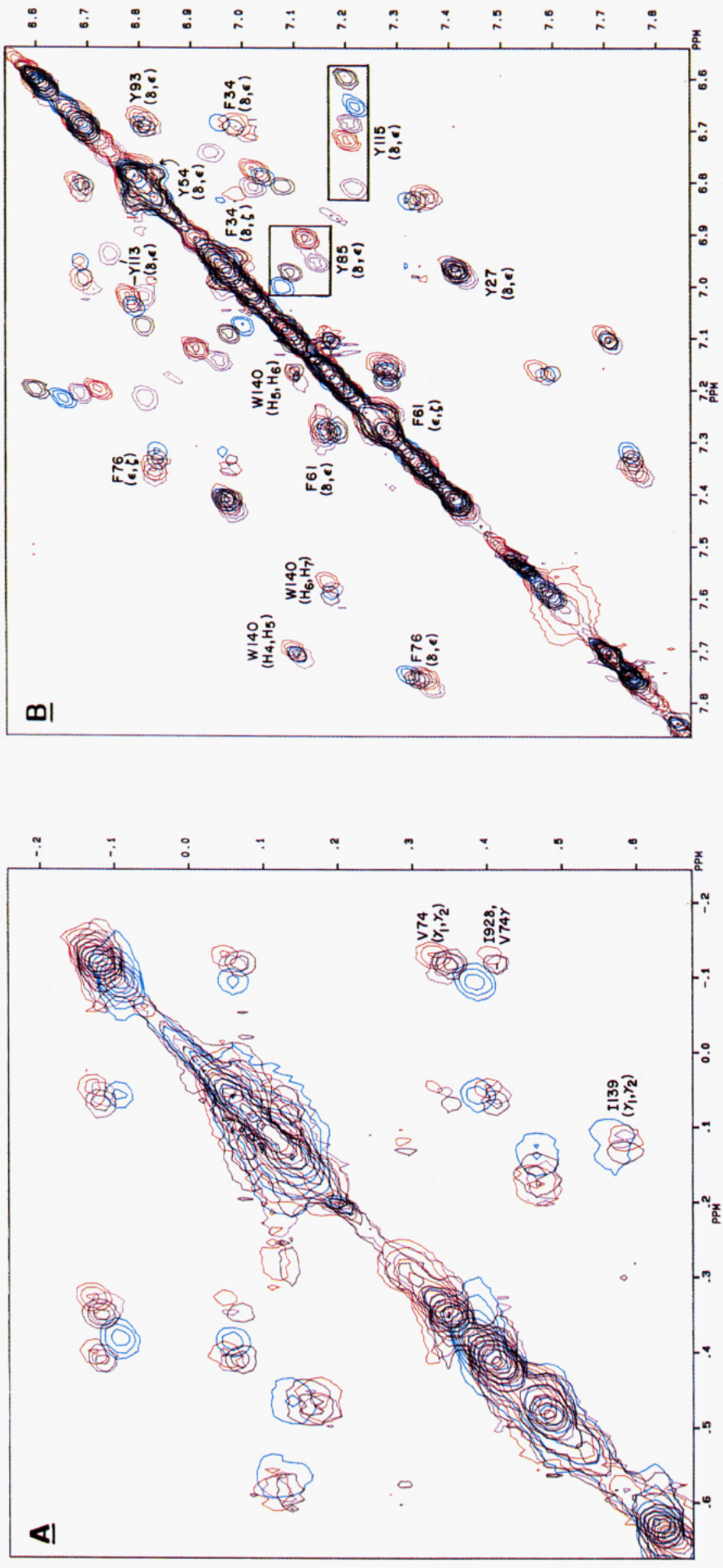

FIGURE 5: 2D ^{1}H NMR (phase-sensitive NOESY) spectra in ^2H_2O of wild-type staphylococcal nuclease and its mutants in the presence of Ca^{2+} and 3′,5′-pdTp. The colors are the same as in Figure 4, and the concentrations and experimental conditions are given under Materials and Methods. (A) The upfield and (B) the downfield aromatic regions are shown. The assignments are based on the sequential assignments made by Torchia et al. (1989) and by Wang et al. (1990). In (B) additional cross peaks are found in the R87G mutant for Tyr-85, Tyr-113, and Tyr-115 (see Results).

Table IV: Metal-Binding Properties of Binary Complexes of Mn^{2+} and Ca^{2+} and Enhancement of Mn^{2+} Complexes[a]

enzyme or ligand	n	K_D^{Mn} or K_I^{Mn} (μM)	ϵ_b[d]	K_D^{Ca} or K_I^{Ca} (μM)
WT	0.95 ± 0.03[b]	416 ± 22[b]		
	1.00 ± 0.05[c]	460 ± 63[c]	8.4 ± 0.7	510 ± 70[e]
E43S	0.85 ± 0.09[b]	3400 ± 180[b]		
	0.75 ± 0.11[c]	3250 ± 300[c]	5.8 ± 0.4	5400 ± 1600[e]
R87G	0.95 ± 0.05[b]	850 ± 83[b]		
	1.02 ± 0.06[c]	958 ± 93[c]	6.0 ± 0.2	4590 ± 280[e]
E43S + R87G	0.89 ± 0.2[b]	6850 ± 3500[b]		
	1.12 ± 0.2[c]	7270 ± 2000[c]	10.5 ± 0.6	26000 ± 5000[e]
3′,5′-pdTp	1.6 ± 0.2[b]	474 ± 50[b]	1.7 ± 0.1	1200 ± 700[f]
5′-pdTdA	1.0 ± 0.1[b]	2000 ± 200[b,c]	2.2 ± 0.1	7260 ± 800[e,f]

[a] n is the stoichiometry of metal binding, K_D is the dissociation constant of the binary enzyme metal complex, K_I is the dissociation constant of the binary metal nucleotide complex, and ϵ_b is the enhancement of the binary Mn^{2+} complex. The parameters for wild-type, R87G, and 3′,5′-pdTp are from Serpersu et al. (1987). The parameters for E43S are from Serpersu et al. (1989), and the parameters for 5′-pdTdA are from Weber et al. (1990b). [b] Determined by EPR as in Figure 6. [c] Determined by $1/T_{1P}$ of water protons, with ϵ_b. [d] Determined by EPR and $1/T_{1P}$ of water protons. [e] Determined by competition with Mn^{2+} measuring $1/T_{1P}$* of water protons (Figure 7A). [f] Determined by competition with Mn^{2+}, measuring free [Mn^{2+}] by EPR (Serpersu et al., 1986).

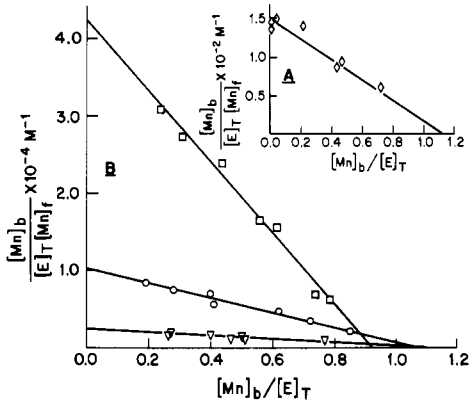

FIGURE 6: Scatchard plots of binary and ternary complexes of mutant staphylococcal nuclease measuring the concentration of free Mn^{2+} by EPR. (A) Binary titration of the double mutant E43S + R87G with Mn^{2+} (◇). The solutions contained either 4.37 or 3.075 mM E43S + R87G. (B) Ternary titrations of E43S + R87G (▽) and E43S (□) with Mn^{2+} in the presence of 5′-pdTdA and of E43S + R87G in the presence of 3′,5′-pdTp (○). The solutions contained 615 μM E43S + R87G and 705 μM 5′-pdTdA (▽), 64.7 μM E43S and 70.5 μM 5′-pdTdA (□), and 586.5 μM R87G + E43S with 615.0 μM 3′,5′-pdTp (○). All solutions contained 40.0 mM Tris-HCl, pH 7.4, T = 23 °C.

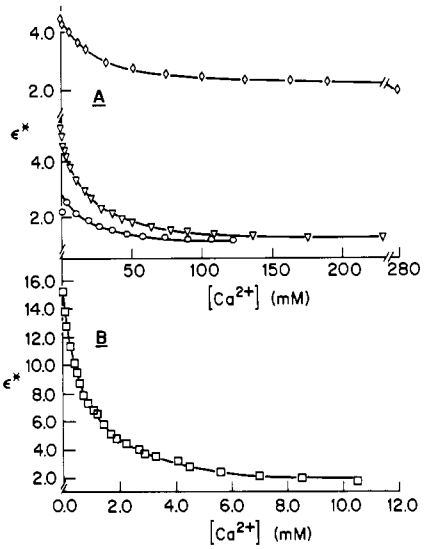

FIGURE 7: Displacement of Mn^{2+} by Ca^{2+} from various binary and ternary complexes of staphylococcal nuclease monitored by changes in the enhancement (ϵ^*) of the effects of Mn^{2+} on $1/T_1$ of water protons. (A) Displacement of Mn^{2+} by Ca^{2+} from complexes of E43S + R87G. The solutions contained 3.63 mM E43S + R87G with 156.5 μM $MnCl_2$ (◇), 615 μM E43S + R87G with 156.5 μM $MnCl_2$ and 705 μM 5′-pdTdA (▽), 146.6 μM E43S + R87G with 156.6 μM $MnCl_2$ and 153.8 μM 3′,5′-pdTp (○). (B) Displacement of Mn^{2+} by Ca^{2+} from the ternary E43S–Mn^{2+}–pdTdA complex. The solution contained 64.7 μM E43S with 23.5 μM $MnCl_2$ and 70.5 μM 5′-pdTdA (□). All solutions contained 40 mM Tris-HCl, pH 7.4, T = 23 °C. For all titrations, Ca^{2+} was added from concentrated stock solutions that also contained all other components of the titration at the same final concentrations. In both (A) and (B) the data points are shown together with best-fit K' curves. The relationship $K^{Ca} = K'/(1 + [Mn^{2+}]/K^{Mn})$ is utilized where K^{Ca} is the calculated dissociation constant for Ca^{2+} from the binary (K_D) or ternary (K_A') complex and K^{Mn} is the previously measured binary or ternary dissociation constant for Mn^{2+} from the same binary or ternary complex (Serpersu et al., 1986).

of $1/T_{1P}$ of water protons, a function of the amount of bound Mn^{2+}, was determined by pulsed NMR. The values for free and bound Mn^{2+} determined by EPR spectroscopy and independently by $1/T_{1P}$ of water protons were analyzed by Scatchard plots exemplified in Figure 6A and compared with K_D^{Mn} values previously determined for the wild-type, the R87G, and the E43S single mutant enzymes (Table IV, Serpersu et al., 1986, 1987, 1989). All enzyme forms show the binding of Mn^{2+} at a single site (Figure 6A, Table IV). While the dissociation constant of Mn^{2+} (K_D^{Mn}) from the R87G mutant is 2.1-fold greater than that from the wild-type enzyme and K_D^{Mn} from the E43S mutant is 7.7-fold greater, K_D^{Mn} from the E43S + R87G double mutant is 16.2-fold greater, which agrees within error with the product of the effects of the two single mutations. Hence the weakening effects on Mn^{2+} binding of the E43S and R87G single mutations are additive in the double mutant, i.e., the interaction energy $\Delta\Delta G_B$ of the effects of the R87G and E43S mutations on K_D^{Mn} is approximately zero (Table II), reflecting independent effects of the two mutations on Mn^{2+} binding.

The addition of Ca^{2+} to the binary Mn^{2+} complex of the E43S + R87G double mutant enzyme decreased the observed enhancement, suggesting that Ca^{2+} displaces Mn^{2+} from the enzyme (Figure 7A). This point was established by EPR, which detected the appearance of free Mn^{2+}, and at high levels of Ca^{2+} essentially all of the Mn^{2+} was displaced. From the amount of Ca^{2+} required to displace half the bound Mn^{2+} and the measured dissociation constant of the binary enzyme–Mn^{2+} complex, a Ca^{2+}–enzyme dissociation constant (K_D^{Ca} = 26 ± 5 mM) was determined for the double mutant E43S + R87G (Table IV). These K_D values were used to calculate a curve that fit the data, assuming simple competition between Mn^{2+}

Table V: Dissociation Constants (μM) and Enhancement Factors in Ternary Enzyme–Metal–3′,5′-pdTp Complexes of Wild-Type and Mutant Staphylococcal Nuclease[a]

complex	enzyme	K_A' EPR	K_A' $1/T_{1P}$[b]	K_S[c,d] $1/T_{1P}$	K_3[d] $1/T_{1P}$	K_2 $1/T_{1P}$	ϵ_T
enzyme–Mn^{2+}–3′,5′-pdTp	WT	11 ± 0.6	17.0 ± 2.0	95 ± 30[e]	2.5 ± 1.0	2.2 ± 0.9	24.8 ± 0.4
	E43S	14.6 ± 0.7	8.0 ± 0.8	66 ± 17	0.22 ± 0.06	1.6 ± 0.5	22.0 ± 2.7
	R87G	117 ± 9.0	175 ± 44	58 ± 17	7.2 ± 1.9	13.0 ± 4.0	7.0 ± 0.8
	E43S + R87G	120 ± 16	105 ± 10	70.4 ± 3.0	1.02 ± 0.2	16.7 ± 5.0	4.84 ± 0.7

complex	enzyme	$K_A'^{Ca}$[e]	K_S	K_3^{Ca}[f]	K_2^{Ca}[g]
enzyme–Ca^{2+}–3′,5′-pdTp	WT	71 ± 8	95 ± 30	13.1 ± 5.8	5.6 ± 1.9
	E43S	228 ± 70	66 ± 17	2.8 ± 0.8	12.6 ± 8.9
	R87G	1420 ± 380	58 ± 17	16.2 ± 5.9	62.1 ± 43
	E43S + R87G	7266 ± 1680	70.4 ± 3.0	19.7 ± 5.9	426 ± 131

[a] The dissociation constants of the ternary and of the relevant binary complexes of enzyme (E), metal (M), and ligands (L) are defined as follows (Mildvan & Cohn, 1966): K_1 = [M][L]/[M–L]; K_D = [E][M]/[E–M]; K_2 = [E][M–L]/[E–M–L]; K_A' = [E–L][M]/[E–M–L]; K_3 = [E–M]-[L]/[E–M–L]; K_S = [E][L]/[E–L]. Note that $K_1K_2 = K_3K_D = K_A'K_S$. All parameters for wild-type and R87G are from Serpersu et al. (1987). All parameters for E43S are from Serpersu et al. (1989). [b] Determined by $1/T_{1P}$* of water protons in Mn^{2+} titrations. [c] Determined by Serpersu et al. (1987) utilizing an increase in fluorescence of 3′,5′-epAp when it was displaced by 3′,5′-pdTp and by computer analysis of nucleotide titrations. [d] Determined by computer analysis of nucleotide titrations (Figure 8) (Reed et al., 1970; Mildvan & Engle, 1972). [e] Determined by competition with Mn^{2+} measuring $1/T_{1P}$* of water protons (Figure 7A). [f] Based on $K_A'K_S/K_D$ (Table IV). [g] Based on $K_A'K_S/K_1$ (Table IV).

and Ca^{2+} at a single site on the enzyme (Figure 7A). As found with Mn^{2+}, the effects of the R87G and D21E single mutations on the dissociation constant of Ca^{2+} were additive in the double mutant (Tables II and IV). These results suggest that the residues Arg-87 and Glu-43 act independently to facilitate the binding of divalent cations by the wild-type enzyme.

Ternary Enzyme–Metal–3′,5′-pdTp Complexes of the E43S + R87G Double Mutant. The thermodynamics of a ternary system of enzyme, metal, and nucleotide is described by six equilibrium constants, which are defined in Table V. The dissociation constant of the binary Mn^{2+} complex of the substrate analogue 3′,5′-pdTp (K_1) was previously determined (Serpersu et al., 1986), and those of the binary Mn^{2+}–enzyme complexes (K_D) were determined by EPR and by $1/T_1$ measurements (Table IV). To determine K_A', the dissociation constant of Mn^{2+} from the ternary enzyme–Mn^{2+}–nucleotide complex, the double mutant E43S + R87G, in the presence of an equivalent amount of 3′,5′-pdTp, was titrated with Mn^{2+}, measuring the free Mn^{2+} by EPR and independently the effects of bound Mn^{2+} on $1/T_1$ of water protons, and the data were analyzed by Scatchard plots (Figure 6B). The K_A' values (Table V) indicate that the R87G mutation weakens Mn^{2+} binding in the ternary 3′,5′-pdTp complex by a factor of 10 ± 2; the E43S mutation has no significant effect; and the double mutant weakens Mn^{2+} binding by a factor of 8 ± 1. Formally, the double mutant thus shows additive effects of the two single mutations on K_A' (Mn^{2+}, pdTp) as well as no additional effects of the second mutation on the first in the double mutant since both $\Delta\Delta G_A$ and $\Delta\Delta G_B$ are zero (Table II). This ambiguity does not exist for K_A' (Ca^{2+}, pdTp) (vide infra).

K_3 (Mn^{2+}, pdTp), the dissociation constant of the inhibitor 3′,5′-pdTp from the ternary enzyme–Mn^{2+}–3′,5′-pdTp complex of the double mutant was determined by titrations of solutions of enzyme and Mn^{2+} with the nucleotide measuring changes in the enhancement (ϵ*) of $1/T_{1P}$ of water protons (Mildvan & Engle, 1972). The data were fit by computed curves (Figure 8A) yielding the K_3 and K_S values given in Table V. While the R87G mutation weakens the binding of 3′,5′-pdTp 2.9-fold, the E43S mutation tightens it 11-fold and these opposing effects on K_3 (Mn^{2+}, pdTp) are additive in the double mutant (Tables II and V).

The dissociation constant K_S of the binary enzyme–3′,5′-pdTp complex showed no significant effects of either the R87G or E43S single mutations or of the double mutation (Table V). Hence the combination of these mutations induced no new

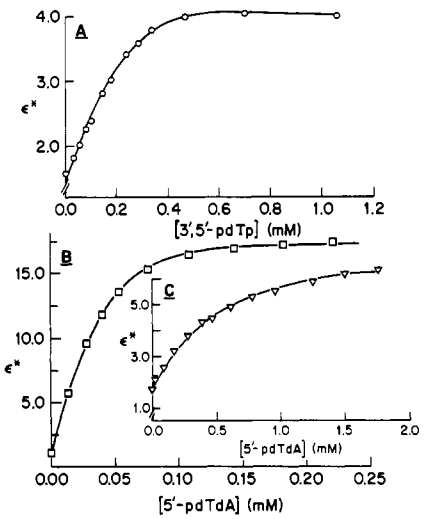

FIGURE 8: Titrations of Mn^{2+} complexes of E43S + R87G and E43S with 5′-pdTdA or 3′,5′-pdTp, measuring the changes in enhancement (ϵ*) of the paramagnetic effects of Mn^{2+} on the $1/T_1$ of water protons. (A) Titration of the double mutant E43S + R87G with 3′,5′-pdTp. The solution contained 586.5 μM E43S + R87G with 156.6 μM $MnCl_2$ (○). (B) Titrations of the mutants E43S + R87G (▽) and E43S (□) with 5′-pdTdA. The solutions contained 615 μM E43S + R87G with 78.3 μM $MnCl_2$ (▽) or 64.7 μM E43S with 43.0 μM $MnCl_2$ (□). All solutions contained 40 mM Tris-HCl, pH 7.4, T = 23 °C.

effect in the double mutant, and no further analysis could be made of K_S (pdTp).

K_A' (Ca^{2+}, pdTp), the dissociation of Ca^{2+} from the ternary enzyme–Ca^{2+}–3′,5′-pdTp complex of the double mutant was determined by competition with Mn^{2+} by monitoring the decrease in the enhancement (ϵ*) of $1/T_{1P}$ of water protons (Figure 7A) and the appearance of free Mn^{2+} by EPR (not shown). The K_A' values indicate (Tables II and V) that the R87G and E43S single mutations weaken Ca^{2+} binding by 1.8 ± 0.2 kcal/mol and 0.7 ± 0.2 kcal/mol, respectively, while the double mutant weakens Ca^{2+} binding by 2.7 ± 0.2 kcal/mol, showing simple additivity of the individual effects.

The dissociation constant of 3′,5′-pdTp from the ternary Ca^{2+} complex K_3 (Ca^{2+}, pdTp) calculated from the ratio of the measured values $K_A'K_S/K_D^{Ca}$ (Table V) is unaffected by the R87G mutation, tightened 4.7 ± 2.0-fold by the E43S mutation, and unaffected by the R87G + E43S double mutation. Hence no additional effect of the E43S mutation on the R87G mutation is detected on K_3 (Ca^{2+}, pdTp) of the double mutant ($\Delta\Delta G_A \sim 0$), and the two residues interact

Table VI: Dissociation Constants (μM) and Enhancement Factors in Ternary Enzyme–Metal–5′-pdTdA Complexes of Wild-Type and Mutant Staphylococcal Nuclease[a]

complex	enzyme	K_A' EPR	K_A' $1/T_{1P}$[b]	K_S[c]	K_3[c]	K_2[c]	ϵ_T[c]
enzyme–Mn^{2+}–5′-pdTdA	WT	6.3 ± 0.1	6.3 ± 0.1	44.7 ± 1.1	0.667 ± 0.02	0.14 ± 0.01	21.8 ± 0.8
	E43S	21.5 ± 1.9	18.4 ± 1.8	33.9 ± 8.3	0.206 ± 0.05	0.34 ± 0.05	26.3 ± 0.6
	R87G	382 ± 40	275 ± 54	233 ± 63	71.8 ± 18	32.4 ± 8.0	10.7 ± 0.5
	E43S + R87G	319 ± 71	450 ± 93	1759 ± 526	84.9 ± 28	298 ± 120	16.4 ± 1.6

complex	enzyme	$K_A'^{Ca}$[d]	K_S	K_3^{Ca}[e]	K_2^{Ca}[f]
enzyme–Ca^{2+}–5′-pdTdA	WT	63.4 ± 6	44.7 ± 1.1	5.56 ± 0.6	0.39 ± 0.05
	E43S	433 ± 87	33.9 ± 8.3	2.72 ± 1.1	2.02 ± 0.3
	R87G	1830 ± 290	233 ± 63	93 ± 25	58.7 ± 16
	E43S + R87G	10880 ± 2000	1759 ± 526	736 ± 292	2636 ± 970

[a] The dissociation constants of the ternary and relevant binary complexes of enzyme, metal, and ligands are defined in Table V. All parameters for WT and R87G are from Weber et al. (1990b). [b] Determined by $1/T_{1P}$* of water protons in Mn^{2+} titrations. [c] Determined by computer analysis of nucleotide titrations (Reed et al., 1970; Mildvan & Engle, 1972). [d] Determined by competition with Mn^{2+}, measuring $1/T_{1P}$* of water protons. [e] Based on $K_A'K_S/K_D$ (Table IV). [f] Based on $K_A'K_S/K_1$ (Table IV).

slightly to weaken the binding of 3′,5′-pdTp in the ternary Ca^{2+} complex of the wild-type enzyme ($\Delta\Delta G_B$ = 1.0 ± 0.8 kcal/mol, Table II).

Ternary Enzyme–Metal–5′-pdTdA Complexes of the E43S + R87G Double Mutant. To further probe the active site of staphylococcal nuclease, complexes of the substrate, 5′-pdTdA, were studied with the same methodology. The K_A' of Mn^{2+} from the ternary enzyme–Mn^{2+}–5′-pdTdA complex of the double mutant 385 ± 117 μM (Figure 6B, Table VI) was found to be 61-fold greater than that of the wild-type enzyme (6.3 ± 0.1 μM) and indistinguishable from K_A' for the single mutant R87G (328 ± 73 μM). Hence the E43S mutation, which by itself weakens K_A' by a factor of 3.2, has had no additional weakening effect on K_A' in the double mutant beyond that produced by the R87G mutation, i.e., $\Delta\Delta G_A \sim 0$ (Table II). The interaction energy $\Delta\Delta G_B$ = −0.6 ±0.3 kcal/mol may reflect cooperativity in Mn^{2+} binding in the ternary complex of the wild-type enzyme facilitated by Arg-87 and Glu-43. In the same ternary complex, no additional effect of the E43S mutation was also observed on the dissociation constant of the substrate, K_3 (Mn, pdTdA) (Figure 8B and Tables II and VI).

The active ternary Ca^{2+} complexes of the substrate, 5′-pdTdA, showed significantly different behavior. These were studied by Mn^{2+} displacement titrations (Figure 7B) before significant amounts of hydrolysis of 5′-pdTdA occurred (<5%), as determined by thin-layer chromatography (Weber et al., 1990b). While the effects of the R87G and E43S mutations on the dissociation constant of Ca^{2+} from the ternary complex K_A' (Ca^{2+}, pdTdA) show simple additivity in the double mutant, the dissociation constant of the substrate K_3 (Ca^{2+}, pdTdA) from this complex shows synergistic weakening effects of the two mutations (Table VI). The amount of synergy, measured by $\Delta\Delta G_B$, is 1.6 ± 0.5 kcal/mol (Table II). Comparable synergistic effects of the two mutations are observed on the dissociation constants (K_2) of Ca^{2+}–5′-pdTdA and Mn^{2+}–5′-pdTdA from their respective ternary complexes and on the dissociation constant (K_S) of the binary enzyme–5′-pdTdA complex (Tables II and VI). As pointed out previously (Weber et al., 1990b), such synergistic effects may reflect strain in the binding of the substrate by the wild-type enzyme, and $\Delta\Delta G_B$ measures the amount of strain.

Discussion

As previously observed (Weber et al., 1990b), the quantitative effects of two mutations of an enzyme may interact differently in a double mutant, depending on which kinetic or thermodynamic parameter of the enzyme is measured. In the present case, the important general acid and base catalysts on staphylococcal nuclease, Arg-87 and Glu-43, were inactivated separately by the R87G and E43S single mutations and simultaneously in the E43S + R87G double mutant. As summarized in Table II, examples of each of the five possible categories of interaction of the two mutations were observed.

Although the wild-type and all of the mutant enzymes were at least 99% folded in the absence of GnHCl (Table III), the denaturation studies revealed antagonistic effects of the E43S and R87G mutations on the stability of the wild-type enzyme, as reflected in K_{app}, the apparent equilibrium constant for denaturation (Table II). Presumably these antagonistic effects on stability result from antagonistic structural effects of the two mutations. This structural antagonism is reflected phenomenologically in the CD spectra (Figure 3), which reveal slight differences in the secondary structures of the R87G and E43S mutants from that of the wild-type enzyme but little or no difference in the double mutant. However, the small differences in the CD spectra are not reflected in the estimated helical content of the mutant enzymes.

Structural antagonism of these two mutations is also reflected in the NMR spectra (Figures 4 and 5), which reveal small differences in the mobility of several aromatic side chains of the R87G mutant from wild-type but no such differences in the E43S single mutant or in the E43S + R87G double mutant.

The profoundly damaging effects of the two single mutations on V_{max} were partially additive in the double mutant, departing from simple additivity by −3.4 kcal/mol (Table II). With the enzyme ketosteroid isomerase, simple additivity of the damaging effects on k_{cat} of mutating the general acid and base catalysts was observed (Kuliopulos et al., 1990), reflecting the independent functioning of these two residues in the concerted, rate-limiting enolization step (Xue et al., 1990). In the case of staphylococcal nuclease, three possible explanations for the departure from simple additivity may be considered: kinetic complexity, antagonistic effects on the structure of the transition state, and cooperative functioning of the general acid and base catalysts to bind the transition state (Weber et al., 1990b; Kuliopulos et al., 1990). Partially additive effects on k_{cat} can be shown mathematically to occur if each single mutation affects the rate of separate consecutive steps in an enzyme–substrate complex, neither of which is rate-limiting (Kuliopulos et al., 1990). In the active ternary staphylococcal nuclease–Ca^{2+}–DNA complex, DNA hydrolysis, facilitated by Arg-87 and Glu-43, occurs by an associative mechanism (Figure 1) the rate of which determines V_{max} (Weber et al., 1990a). No evidence for a long-lived trigonal-bipyramidal

intermediate was detected on the R87G mutant (<1% of the enzyme) by high-field ^{31}P NMR at 242.9 MHz (Weber et al., 1990b), suggesting that concerted rather than stepwise general acid–base catalysis by Arg-87 and Glu-43 constitutes the rate-limiting step that determines V_{max}, i.e., that only a single chemical step is involved. Since the single R87G and E43S mutations would make this step even more rate limiting, kinetic complexity involving separate effects on consecutive non-rate-limiting steps is an unlikely explanation for the partially additive effects of these two mutations.

Similarly, while antagonistic effects of the R87G and E43S mutations on the structure of the ground state of the enzyme are detected by denaturation studies, by both CD and NMR spectroscopy, these effects are very small, and when quantified, as in the free energy of folding (Tables II and III), show much less departure from additivity (−0.7 kcal/mol) than does V_{max} (−3.4 kcal/mol). However, since extrapolation of these small ground-state effects to the transition state cannot be made, larger antagonistic effects on the structure of the transition state cannot be totally excluded.

A more likely explanation for the partially additive effects on V_{max}, which is consistent with a single rate-limiting step and with the high catalytic power of staphylococcal nuclease, is cooperative binding of the transition state by both Arg-87 and Glu-43 (Figure 1). Each single mutation, R87G or E43S, abolishes both the noncooperative interaction of the mutated residue and the cooperative interaction of both residues with the transition state. The double mutation abolishes the noncooperative interactions of both residues with the transition state but abolishes the cooperative interaction only once. Hence the difference in free energy, $\Delta\Delta G^{\ddagger}_{B}$, between the effects of the double mutant and the sum of the effects of the single mutations, −3.4 kcal/mol, measures the cooperative contribution to the binding of the transition state by Arg-87 and Glu-43. The 6.5 kcal/mol kinetic barrier introduced by the R87G mutation may therefore be divided into a 3.4 kcal/mol contribution due to the loss of transition state binding by Arg-87 which is cooperative with that by Glu-43 and a 3.1 kcal/mol contribution due to the loss of noncooperative binding of the transition state by Arg-87 alone. Similarly, the 5.0 kcal/mol barrier introduced by the E43S mutation results from the loss of cooperative (3.4 kcal/mol) and noncooperative (1.6 kcal/mol) binding of the transition state by Glu-43. The cooperative contribution to transition state binding by Arg-87 and Glu-43 thus contributes a factor of $10^{2.5}$ to catalysis.

We next consider the interactions of the effects of the two mutations on metal and substrate binding. Focussing on the catalytically relevant complexes of the enzyme, Ca^{2+}, and the substrate, 5′-pdTdA, it is seen that the damaging effects of the R87G and E43S mutations on Ca^{2+} binding, both in the binary E–Ca^{2+} and ternary E–Ca^{2+}–5′-pdTdA complexes, as reflected in K_D and K_A', respectively, show simple additivity in the double mutant (Table II) indicating that Glu-43 and Arg-87 act independently to facilitate the high-affinity binding of Ca^{2+} by the wild-type enzyme. The Glu-43 residue may do this by direct coordination of Ca^{2+} in the binary complex and by electrostatic interaction in the ternary complex (Serpersu et al., 1989), while Arg-87 may facilitate Ca^{2+} binding by stabilizing the active site structure in the binary complex and by interacting with the substrate in the ternary complex, which, in turn, is directly coordinated by Ca^{2+}. A stabilizing effect of Arg-87 on structure is reflected in the increase in the free energy of folding (Tables II and III) and in the small changes in the CD spectra (Figure 3) and NMR spectra (Figures 4 and 5) of the R87G mutant.

In contrast with the additive effects on Ca^{2+} binding, and the partially additive effects on transition state binding, the R87G and E43S mutations synergistically weaken substrate binding in the double mutant both in the binary enzyme-5′-pdTdA complex as reflected in K_S and in the ternary enzyme–Ca^{2+}–5′-pdTdA complex as reflected in K_3 (Table II). The amount of synergy, measured by $\Delta\Delta G_B$, is 1.4 ± 0.3 kcal/mol in the binary complex and 1.6 ± 0.5 kcal/mol in the ternary complex. The binding of Ca^{2+}–5′-pdTdA in the active ternary complex as reflected in K_2 is also synergistically weakened by the two mutations by 1.3 ± 0.4 kcal/mol (Table II). While synergistic effects alone can be explained by extensive protein unfolding in the double mutant, this explanation is unlikely since denaturation studies, CD, and NMR spectra revealed the double mutant to be native in structure in the absence of denaturant, the tight binding of the substrate analogue 3′,5′-pdTp was largely preserved in the double mutant, and simple additivity of the weakening effects on Ca^{2+} and Mn^{2+} binding was found (Table II). As pointed out previously (Weber et al., 1990b) an alternative explanation for synergistic effects of mutations on ligand binding is strain or anticooperativity in the binding of the ligand by the wild-type enzyme, and the amount of strain in such cases is measured by the amount of synergy, $\Delta\Delta G_B$. In the ternary staphylococcal nculease–Ca^{2+}–5′-pdTdA complex, the catalytic residues Arg-87 and Glu-43 strain the ground state of the enzyme-bound substrates by 1.6 ± 0.5 kcal/mol (Table II). The loss of this strain, as the transition state is approached, may constitute a part of the cooperative contribution to transition state binding by these residues, estimated above as −3.4 kcal/mol.

A structural basis for strain in substrate binding and cooperativity in transition state binding by Glu-43 and Arg-87 may be suggested. Strain in the ground state could result from compression of the attacking water into the reaction center phosphorus between Glu-43 and Arg-87. In the phosphorane transition state, this compression is relieved by bonding of the entering water to phosphorus, which shortens the O–P distance. Since the phosphorane transition state is a single entity, rather than separate water and phosphodiester molecules, its chelation between Glu-43 and Arg-87 is strengthened, resulting in its cooperative binding (Figure 1). This difference between the ground state and the transition state would be even greater if a loosely bound second sphere water molecule were the attacking substrate.

In a similar study of the interactions of the D21E mutation with the R87G mutation, additive weakening effects on the binding of the substrate, 5′-pdTdA, and synergistic weakening effects on the binding of the substrate analogue, 3′,5′-pdTp, were observed (Weber et al., 1990b), different from those found here (Table II). Hence Asp-21, a metal-liganding residue (Figure 1), and Arg-87 interact anticooperatively to introduce strain into the binding of the substrate analogue and act independently to facilitate substrate binding. In contrast, Glu-43, the general base, and Arg-87 interact cooperatively to bind the substrate but act independently in the binding of the analogue. These observations indicate that Arg-87 interacts differently with Asp-21 than with Glu-43 and that the analogue 3′,5′-pdTp, although it occupies the substrate site, differs significantly in its detailed mode of binding from the substrate.

It is concluded that in the active ternary complex of wild-type staphylococcal nuclease, Arg-87 and Glu-43 bind the ground state of the substrate in part anticooperatively, elevating its free energy by 1.6 kcal/mol, and bind the transition

state in part cooperatively, lowering its free energy by −1.8 kcal/mol. The combination of these anticooperative and cooperative effects decreases the kinetic barrier to V_{max} by 3.4 kcal/mol. Acting independently, Arg-87 further lowers the free energy barrier to V_{max} by an additional 3.1 kcal/mol and Glu-43 independently lowers the free energy barrier to V_{max} by an additional 1.6 kcal/mol. The summation of the anticooperative, cooperative, and noncooperative effects of Arg-87 and Glu-43 results in an overall lowering of the kinetic barrier to catalysis by 8.1 kcal/mol due to general acid–base catalysis and transition state stabilization by these two residues. The remaining 13.7 kcal/mol decrease in $\Delta G^{\ddagger}$ may reasonably be ascribed to catalysis by approximation (Jencks, 1975) and to metal catalysis by Ca^{2+}.

ACKNOWLEDGMENTS

We are grateful to Mary A. Mullen and Gary S. Hayward for generously supplying us with plasmid DNA, to David Shortle for providing us with the expression plasmids for the single and double mutants and for valuable discussions, and to Peggy Ford for secretarial assistance.

REFERENCES

Anfinsen, C. B., Cuatrecasas, P., & Taniuchi, H. (1971) *Enzymes 4*, 177–204.

Anil Kumar, Ernst, R. R., & Wüthrich, K. (1980) *Biochem. Biophys. Res. Commun. 95*, 1–6.

Brahms, S., & Brahms, J. (1980) *J. Mol. Biol. 138*, 149–178.

Carr, H. Y., & Purcell, E. M. (1954) *Phys. Rev. 94*, 630–638.

Carter, P. J., Winter, G., Wilkinson, A. J., & Fersht, A. R. (1984) *Cell 38*, 835–840.

Chang, C. T., Wu, C.-S. C., & Yang, J. T. (1978) *Anal. Biochem. 91*, 13–31.

Cohn, M., & Townsend, J. (1954) *Nature (London) 173*, 1090–1091.

Compton, L. A., & Johnson, W. C. (1986) *Anal. Biochem. 155*, 155–167.

Cotton, F. A., Hazen, E. E., & Legg, M. J. (1979) *Proc. Natl. Acad. Sci. U.S.A. 76*, 2551–2555.

Cuatrecasas, P., Fuchs, S., & Anfinsen, C. B. (1967a) *J. Biol. Chem. 242*, 1541–1547.

Cuatrecasas, P., Fuchs, S., & Anfinsen, C. B. (1967b) *J. Biol. Chem. 242*, 4759–4767.

Dunn, B. M., DiBello, C., & Anfinsen, C. B. (1973) *J. Biol. Chem. 248*, 4769–4774.

Fry, D. C., Byler, D. M., Susi, H., Brown, E. M., Kuby, S. A., & Mildvan, A. S. (1988) *Biochemistry 27*, 3588–3598.

Hibler, D. W., Stolowich, J. N., Reynolds, M. A., Gerlt, J. A., Wilde, J. A., & Bolton, P. H. (1987) *Biochemistry 26*, 6278–6286.

Jeener, J., Meier, B. H., Bachmann, P., & Ernst, R. R. (1979) *J. Chem. Phys. 71*, 4546–4553.

Jencks, W. P. (1975) *Adv. Enzymol. Relat. Areas Mol. Biol. 43*, 219–410.

Knowles, J. R. (1987) *Science 236*, 1252–1258.

Kuliopulos, A., Talalay, P., & Mildvan, A. S. (1990) *Biochemistry 29*, 10271–10280.

Kunkel, T. A., Roberts, J. D., & Zakour, R. A. (1987) *Methods Enzymol. 154*, 367–383.

Laemmli, U. K. (1970) *Nature (London) New Biol. 227*, 680–685.

Lachica, R. V. F., Genegeorgis, C., & Hoeprich, P. D. (1971) *Appl. Microbiol. 21*, 585–587.

Loll, P. J., & Lattman, E. E. (1989) *Proteins 5*, 183–201.

Marion, D., & Wüthrich, K. (1983) *Biochem. Biophys. Res. Commun. 113*, 967–974.

Marion, D., & Bax, A. (1988) *J. Magn. Reson. 79*, 352–356.

Mildvan, A. S., & Cohn, M. (1963) *Biochemistry 2*, 910–919.

Mildvan, A. S., & Cohn, M. (1966) *J. Biol. Chem. 241*, 1178–1193.

Mildvan, A. S., & Engle, J. L. (1972) *Methods Enzymol. 49G*, 322–359.

Mildvan, A. S., & Serpersu, E. H. (1989) in *Metal Ions in Biological Systems* (Sigel, H., Ed.) Vol. 25, pp 309–334, Marcel Dekker, Inc., New York.

Mullen, G. P., Shenbagamurthi, P., & Mildvan, A. S. (1989) *J. Biol. Chem. 264*, 19637–19647.

Pourmotabbed, T., Dell'Acqua, M., Gerlt, J. A., Stanczyk, S. M., & Bolton, P. A. (1990) *Biochemistry 29*, 3677–3683.

Reed, G. H., Cohn, M., & O'Sullivan, W. J. (1970) *J. Biol. Chem. 245*, 6547–6552.

Serpersu, E. H., Shortle, D., & Mildvan, A. S. (1986) *Biochemistry 25*, 68–77.

Serpersu, E. H., Shortle, D., & Mildvan, A. S. (1987) *Biochemistry 26*, 1289–1300.

Serpersu, E. H., McCracken, J., Peisach, J., and Mildvan, A. S. (1988) *Biochemistry 27*, 8034–8044.

Serpersu, E. H., Hibler, D. W., Gerlt, J. A., & Mildvan, A. S. (1989) *Biochemistry 28*, 1539–1548.

Shortle, D. (1983) *Gene 22*, 181–189.

Shortle, D. (1986) in *Protein Engineering, Applications in Science, Medicine, and Industry* (Inouye, M., & Sarma, R., Eds.) pp 233–241, Academic Press, Inc., New York.

Shortle, D., & Lin, B. (1985) *Genetics 110*, 539–555.

Shortle, D., & Meeker, A. K. (1986) *Proteins: Struct., Funct., Genet. 1*, 81–89.

Shortle, D., & Meeker, A. K. (1989) *Biochemistry 28*, 936–944.

Shortle, D., Stites, W. E., & Meeker, A. K. (1990) *Biochemistry 29*, 8033–8041.

Stone, A. L., Park, J. Y., & Martenson, R. E. (1985) *Biochemistry 24*, 6666–6673.

Tabor, S., & Richardson, C. C. (1987) *Proc. Natl. Acad. Sci. U.S.A. 84*, 4767–4771.

Torchia, D. A., Sparks, S. W., & Bax, A. (1989) *Biochemistry 28*, 5509–5524.

Wang, J., LeMaster, D. M., & Markley, J. L. (1990) *Biochemistry 29*, 88–101.

Weber, D. J., Lebowitz, M. S., & Mildvan, A. S. (1990a) *FASEB J.*, A1979.

Weber, D. J., Serpersu, E. H., Shortle, D., & Mildvan, A. S. (1990b) *Biochemistry 29*, 8632–8642.

Xue, L., Talalay, P., & Mildvan, A. S. (1990) *Biochemistry 29*, 7491–7500.